The Hydrogen Bonding Interactions between the Ionic Liquid 1-Ethyl-3-Methylimidazolium Ethyl Sulfate and Water

Qing-Guo Zhang,[†,‡] Nan-Nan Wang,[†] and Zhi-Wu Yu*[,†]

Key Laboratory of Bioorganic Phosphorous Chemistry and Chemical Biology (Ministry of Education), Department of Chemistry, Tsinghua University, Beijing 100084, China, and College of Chemistry and Chemical Engineering, Bohai University, Jinzhou 121000, China

Received: November 20, 2009; Revised Manuscript Received: March 7, 2010

1-Ethyl-3-methylimidazolium ethyl sulfate (EMIES) is a novel ionic liquid with potential industrial applications. Attenuated total reflectance infrared spectroscopy, ^{1}H NMR spectroscopy, and quantum chemical calculations were employed to investigate the molecular interactions between water and EMIES. The infrared spectra were analyzed by two methods: excess spectroscopy and two-dimensional correlation spectroscopy. This showed that the hydrogen bond involving the $-SO_3$ group in the ethyl sulfate anion (ES) was enhanced, while those involving the aromatic C−H groups of 1-ethyl-3-methylimidazolium cation (EMI) were weakened in the presence of water. During the process of increasing water concentration, the hydrogen bonding interaction between H_2O and SO is prior to that between H_2O and the C−H group on the imidazolium ring. At low concentrations, water interacts selectively with $-SO_3$ in the ethyl sulfate anion, while, at high concentrations (mole fraction of water equal or greater than 0.6), it can also form hydrogen bonds directly with the imidazolium ring. The following sequential order of interaction strength is established: EMI−water−ES > EMI−ES > ES−water > EMI−water.

1. Introduction

Ionic liquids (ILs) are a family of liquid compounds consisting solely of ions at room temperature. They constitute a remarkably promising class of technologically useful and fundamentally interesting materials[1−6] and provide an attractive alternative to traditional organic solvents for both laboratory and industrial purposes because of their potential as "green" solvent and reaction media.[1−12] Despite tremendous efforts devoted to ILs in recent years, they are still considered as esoteric materials because they are not easily available and are expensive for practical applications. In 2002, Holbrey et al.[12] proposed the use of the common industrial alkylating agent diethyl sulfate for the preparation of the ionic liquid 1-ethyl-3-methylimidazolium ethyl sulfate (EMIES). This IL possesses a number of desirable properties for potential industrial applications: convenient preparation, good thermal stability, unreactive in air/water, and superior in electrochemistry.[13] A number of studies of the properties of EMIES have been published.[14−19]

To expand the applications of ionic liquids, IL-based mixed solvents have come into focus in recent years.[20,21] A particular cosolvent has been the ubiquitous solvent, water. It has been shown that the presence of water and other cosolvents can strongly affect the physical and chemical properties of ionic liquids such as density,[16−18,22] surface tension,[16,17] vapor pressure,[23] viscosity,[18,19] electrical conductivity,[24] heat capacity,[15] extraction capacity,[14] as well as solvation and solubility properties.[25−27]

Hydrogen bonds are believed to play an important role in the interaction between ILs and cosolvents.[28,29] Some studies focused on hydrogen bonds[28−38] have been carried out to understand the properties of ILs and structural changes induced when mixed with other solvents. Seddon's group was the first to report the existence of hydrogen bonds in imidazolium salts.[28] Voth and co-workers investigated the nanostructural organization in [Omim]−nitrate IL and water mixtures by MD simulations. They found that the most ordered micelle (cation−cation) structure and water (water−anion−water) network were formed at certain turnover points during dilution with water.[29] Takamuku et al. investigated the state of water in the IL 1-ethyl-3-methylimidazolium tetrafluoroborate (EMIBF$_4$), and suggested that the state of water molecules in EMIBF$_4$ significantly changes at $x_w \approx 0.3$.[30] Ludwig's group performed several studies on hydrogen bonds in ILs,[4,5,31−33] and found strong and directional H-bonds are formed between cations and anions which can fluidize ionic liquids by destroying the symmetry of charge.[5] Li's group[34] investigated the properties of the mixtures of deuterated dimethyl sulfoxide (DMSO-d_6) and 1-butyl-3-methylimidazolium tetrafluoroborate ([Bmim][BF$_4$]) by IR and quantum chemical calculations. They found that hydrogen bonds formed with the nearby functional group of the cation contributed significantly to the blue-shifted C−D stretching vibrations of DMSO-d_6.

Water−IL interactions when ILs contain sulfate-based anions are of particular interest to us. There have been a few publications with either fixed water content or limited water concentration range. Chang et al. found that the structure of pure 1,3-dimethylimidazolium methyl sulfate was appreciably changed through hydrogen bonds with water at x (water) = 0.9.[35] Ludwig and co-workers investigated the IL EMIES mixed with low water content up to 1 wt % H_2O/D_2O through FTIR and DFT calculation, demonstrating that water molecules are mainly H-bonded to the IL anions.[4] In another study, Cammarata et al. were the first to report that most of the water molecules exist in symmetric 1:2 type H-bonded complexes with several anions of imidazolium-based ILs involving the $[CF_3SO_3]^-$ anion at low

* To whom correspondence should be addressed. Phone: (+86) 10 6279 2492. Fax: (+86) 10 6277 1149. E-mail: yuzhw@tsinghua.edu.cn.
† Tsinghua University.
‡ Bohai University.

10.1021/jp1009498
Published on Web 03/25/2010

water concentration and using D_2O in the study of IL−water interaction.[36] Similar conclusions were approved by Porter et al. using molecular dynamic simulation.[37]

Hydrogen bonding interactions between water and a sulfate-containing IL like EMIES, however, have not been reported in the whole concentration range. To exploit our experience of studies of hydrogen bonds in liquid binary systems,[39−42] we have investigated the hydrogen bonding properties and dynamic interaction properties of EMIES−water binary systems using ATR-IR, ^{1}H NMR, and density functional theory (DFT) calculation. In particular, excess infrared absorption spectroscopy[41−43] and two-dimensional (2D) correlation spectroscopy have been employed to reveal details of the molecular interactions. The former was developed in our laboratory by applying the idea of excess thermodynamic functions to spectroscopy which can enhance spectral resolution and estimate molecular interactions in liquid solutions.[39−42] The latter can provide information on the sequential order and the dynamic properties of interaction during the mixing process.[44−50]

2. Experimental Section

2.1. Chemicals. EMIES was synthesized according to Holbrey's method.[12] The product obtained is a colorless ionic liquid. The ^{1}H NMR chemical shifts of EMIES are as follows: δ_H (300 MHz, no solvent), 0.7966 (3H, t, $NCCH_3$), 1.1491 (3H, t, $OCCH_3$), 3.5539 (3H, s, NCH_3), 3.7038 (2H, q, OCH_2), 3.9900 (2H, q, NCH_2), 7.4878 (1H, s, C4−H), 7.5976 (1H, s, C5−H), 8.8326 (1H, s, C2−H). These data are in good agreement with the literature.[12] The electrochemical window of EMIES was measured by cyclic voltammetry at 303.15 K. The result showed reductive and oxidative limits of −1.40 and 2.40 V, respectively, relative to an Al/Al^{3+} reference. This gave an electrochemical potential window of 3.8 V, the same as the published works.[12,51] Deionized water was distilled in quartz still with a conductivity of $(0.9−1.3) \times 10^{-4}$ S·m^{-1}. D_2O was purchased from Aldrich (99.9 atom % D).

2.2. Sample Preparation. A series of EMIES−H_2O and EMIES−D_2O binary mixtures were prepared by weighing. The mole fractions of H_2O in EMIES−H_2O mixtures are 0.0846, 0.2010, 0.2995, 0.3942, 0.4962, 0.5996, 0.6977, 0.8009, and 0.9014. The mole fractions of D_2O in EMIES−D_2O mixtures are 0.0991, 0.2115, 0.3071, 0.4038, 0.4980, 0.5978, 0.6982, 0.8011, and 0.9014.

2.3. FTIR Spectroscopy. FTIR spectra over the range from 4000 to 650 cm^{-1} were collected at room temperature (~25 °C) using a Nicolet 5700 FTIR spectrometer, equipped with a DTGS detector. Two attenuated total reflection (ATR) cells were employed in the experiments. They are made of trapezoidal ZnSe/Ge crystals with incident angles of 45°/60° and 12/7 reflections. The Ge crystal, with fewer numbers of reflections and thus shorter effective light path, was used to examine the strong stretching bands of $-SO_3$. Spectra were recorded with a resolution of 2 cm^{-1} and a zero filling factor of 2, 16 parallel scans. Three parallel measurements for each sample were carried out. The refractive indexes of solutions were measured with a refractometer at 25 °C. The formulas suggested by Hansen[52] were used to do the ATR corrections.

2.4. Excess Absorption Spectroscopy. The theory of excess absorption spectroscopy has been described in detail elsewhere.[41,42] Briefly, an excess infrared absorption spectrum is defined as the difference between the spectrum of a real solution and that of the respective ideal solution under identical conditions. The working equation in calculating the excess infrared absorption spectrum is

$$\varepsilon^E = \frac{A}{d(C_1 + C_2)} - (x_1\varepsilon_1^* + x_2\varepsilon_2^*) \quad (1)$$

where A is the absorbance of the mixture, d is the light path length, C_1 and C_2 are the molarities of the two components, x_1 and x_2 are the mole fractions of components 1 and 2, and ε_1^* and ε_2^* are the molar absorption coefficients of the two components in their pure states, respectively.

The calculation of the excess infrared spectra was programmed using Matlab 7.0 (Math Works Inc., Natick, MA). The data manipulations, i.e., the subtraction, truncation, and baseline correction of the IR spectra, were also performed using Matlab 7.0.

2.5. 2D IR Correlation Analysis. Standard 2D correlation calculation was performed using Matlab 7.0, based on the algorithm developed by Noda.[45] The average spectrum of all of the spectra over the full concentration range was used as the reference spectrum. In the 2D correlation contour map, solid and dashed lines represent positive and negative correlation intensities, respectively.

2.6. ^{1}H NMR Measurements. The ^{1}H NMR spectra of samples were obtained on a JEOL JNM-ECA 300 NMR spectrometer (300 MHz) at 298 K with TMS as the internal standard.

2.7. Quantum Chemical Calculations. The geometries, binding energies, harmonic vibrational frequencies, and IR intensities were obtained by the density functional theory (DFT) at the 6-31++G(d,p) basis set with the Gaussian 03 program.[53] DFT has been used extensively to study the interactions between ionic liquids and cosolvents such as water, acetone, and DMSO.[33,34,54−56] We selected the 6-31++G** basis set in our calculation following those studies. The optimized geometries were recognized as local minima with no imaginary frequency.

3. Results and Discussion

3.1. ATR and Excess Infrared Spectra Analysis. The chemical structure and atom numbering for EMIES is described in Figure 1. The ATR-IR spectra of pure EMIES, H_2O, and D_2O are shown in Figure 2. Clearly, the use of D_2O can avoid the overlap of certain bands of water and the IL. The assignments of the stretching vibrations of the main functional groups C−H, C=C, C=N, and $-SO_3$ in pure EMIES are based on a comparison between the observed and calculated frequencies/wavenumbers of the respective vibration modes. The results are listed in Table 1. The scaling factor for the calculated frequencies is 0.955.[35,44] The bands observed above 3040 cm^{-1} are attributed to the C−H stretching vibrations on the imidazolium ring. The vibrational band at wavenumber 3150 cm^{-1} is attributed to C4,5−H stretching modes and that at 3104 cm^{-1} to C2−H stretching modes.[33,57] The bands in the range 3040−2900 cm^{-1} can be assigned to the alkyl ($-CH_3$ and $-CH_2CH_3$) stretching vibrations. The bands observed at 1678, 1574, 1221, and 1018 cm^{-1} are attributed to C=C, C=N, asymmetric $-SO_3$, and symmetric $-SO_3$ stretching vibrations in pure EMIES, respectively. The assignments resemble those given by Kiefer et al. who reported first the IR and Raman spectra of EMIES.[57]

To get a general impression of the influence of water on the vibrational spectra of the main functional groups in EMIES, a preliminary experiment in which pure EMIES was spread on ZnSe or Ge ATR crystals and exposed to air (25 °C, relative humidity 50%) for more than 15 h was examined. A series of IR spectra were collected as a function of time. The continued increase in the absorbance of −OH stretch band around 3500

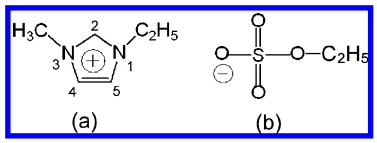

Figure 1. Chemical structure of 1-ethyl-3-methylimidazolium cation (a) and ethyl sulfate anion (b).

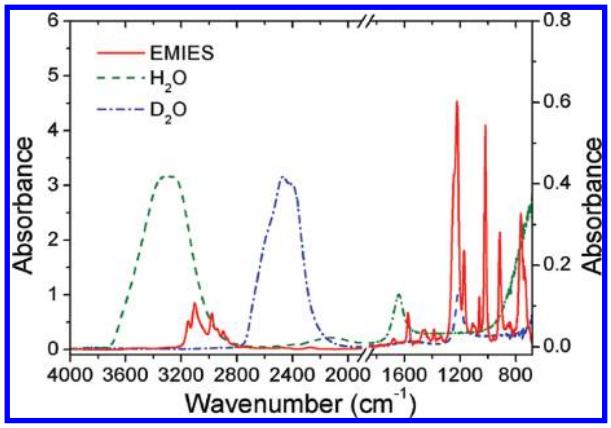

Figure 2. ATR-IR spectra of EMIES, H_2O, and D_2O determined with ZnSe (in the range 4000−1900 cm^{-1}, left absorbance axis) and Ge (in the range 1850−680 cm^{-1}, right absorbance axis) ATR crystals.

TABLE 1: Observed and DFT-Calculated Frequencies of the C−H, C═C, C═N, and S═O Stretching Vibrations in EMIES

frequencies (cm^{-1})		
observed	calculated[a]	assignments
3150	3165 (2)	sym. C4,5−H stretch
	3148 (6)	asym. C4,5−H stretch
3104	3043 (313)	C2−H stretch
2980	3023 (6)	asym. (N)−CH_3 stretch
	3009 (0)	asym. (N)−CH_2CH_3 stretch
	3007 (12)	asym. (N)−CH_3 stretch
	2995 (4)	asym. (N)−CH_2CH_3 stretch
	2988 (34)	asym. (O)−CH_2CH_3 stretch
	2975 (18)	asym. (N)−CH_2CH_3 stretch
	2973 (32)	asym. (O)−CH_2CH_3 stretch
	2948 (8)	asym. (O)−CH_2CH_3 stretch
2943	2934 (33)	sym. (N)−CH_2− stretch
	2921 (58)	sym. (N)−CH_3− stretch
2899	2907 (31)	sym. (O)−CH_2CH_3 stretch
	2905 (47)	sym. (N)−CH_2CH_3 stretch
	2905 (23)	sym. (O)−CH_2CH_3 stretch
1678	1536 (21)	C═C stretch
1574	1528 (50)	C═N stretch
1221	1161 (284)	asym. SO_3 stretch
1018	940 (269)	sym. SO_3 stretch

[a] Calculated frequencies are scaled by 0.955. Data in parentheses are infrared intensities in km/mol.

cm^{-1} indicates that water uptake occurs for about 5 h. The spectrum at this time is about the same as that observed for an aqueous EMIES sample at mole fraction $x(H_2O) = 0.6$. The variations of the absorption bands of −OH, C4,5−H, C2−H, alkyl, and $-SO_3$ stretching vibrations during the hydration process are presented in Figure 3. An immediate and apparent conclusion is that the $-SO_3$ group is significantly affected.

Next, ATR-IR spectra of binary mixtures of EMIES−D_2O and EMIES−H_2O were recorded over the whole concentration range (mole fraction increment of about 0.1) and analyzed by the excess spectroscopy method. Both protonated and deuterated water systems were studied in order to avoid overlap between the C−H and O−H stretching bands in the EMIES−H_2O system and overlap between the S═O stretching and O−D bending in the EMIES−D_2O system. The ATR-IR spectra and excess spectra of the binary mixtures at different water concentrations over the wavenumber range 3300−950 cm^{-1} are shown in Figure 4. In the ATR-IR spectra (Figure 4a−c), ν(C2−H), ν(C4,5−H), and ν(O−D) show a blue shift, while ν(C═C), $\nu_s(-SO_3)$, and $\nu_{as}(-SO_3)$ show a red shift upon addition of water. The wavenumber values of the shifts are given in Figure 5a. In Figure 4b, the band position of ν(C═N) is nearly fixed, but a new band located at 1551 cm^{-1} appears when $x(H_2O) \geq 0.6$. Furthermore, there is an isosbestic point at 1557 cm^{-1} in the ATR-IR spectra of ν(C═N) (Figure 4b). The new band and the isosbestic point suggest the existence of a new interacting complex. This new band is assigned tentatively to the direct interacting complex of water and the 1-ethyl-3-methylimidazolium cation of EMIES. Further discussion will be developed in the later sections.

Excess spectra can reveal the positions of new complexes and the changes in molar absorptivity directly, reflecting details of the molecular interactions in the mixtures. In Figure 4d, with increasing water concentration, the stretching vibration of C2−H and C4,5−H in imidazolium rings has a positive band at the higher wavenumber and negative bands at the lower wavenumber, attributed to the blue shift of the corresponding bands. The stretching vibration of O−D also has a positive band at the higher wavenumber and a negative band at the lower wavenumber, attributed again to the blue shift of the corresponding bands upon dilution.

According to published data,[5,35] there are weak C−H···anion hydrogen bonds in EMIES and EMIES−solvent systems. They are classified as proper red-shift H-bonds,[34,58] and so are the O−D H-bonds.[58] This means that the red shifts of C−H and O−D stretching vibration bands represent the weakening of these bonds and the strengthening of hydrogen bonding interactions between them and proton acceptors. Now that we observed blue shifts of C2−H and C4,5−H in imidazolium rings upon the dilution process, this implies that water weakens the C−H···anion hydrogen bonding interactions of EMIES. Further, the blue shift of C2−H is 14 cm^{-1} and that of C4,5−H is merely 4 cm^{-1} (Figure 5a), indicating that the former has been subjected to a bigger influence upon dilution. This can be attributed to the stronger hydrogen bond of C2−H···anion than that of C4,5−H···anion.[5] Similarly, we can deduce that the hydrogen bonds between D_2O and the cation/anion of EMIES are weaker than the cooperative hydrogen bonds in pure water based on the blue shift of the O−D stretching vibration.

Furthermore, in Figure 4e, the stretching vibration of C═C has a negative band at the higher wavenumber and a positive band at the lower wavenumber, attributed to a red shift of the band. For ν(C═N), there are only some small negative bands at a low concentration of water, but it shows an obvious positive band when $x(H_2O) \geq 0.6$, indicating the imidazolium ring may undergo a different interaction mode with the increase of water content above this level. This implies direct interactions between water and the 1-ethyl-3-methylimidazolium cation of EMIES when $x(H_2O) \geq 0.6$, which is supported by theoretical calculation, as will be discussed in a later section. In Figure 4f, both $\nu_s(-SO_3)$ and $\nu_{as}(-SO_3)$ have a negative band at the higher wavenumber and a positive band at the lower wavenumber, which are attributed to red-shift of these bands. Since the red shift of $\nu_s(-SO_3)$ and $\nu_{as}(-SO_3)$ represent the weakening of the S═O bond and the strengthening of the corresponding hydrogen bond it participates in,[59] the above results indicate that the hydrogen bond S═O···H is enhanced in the dilution

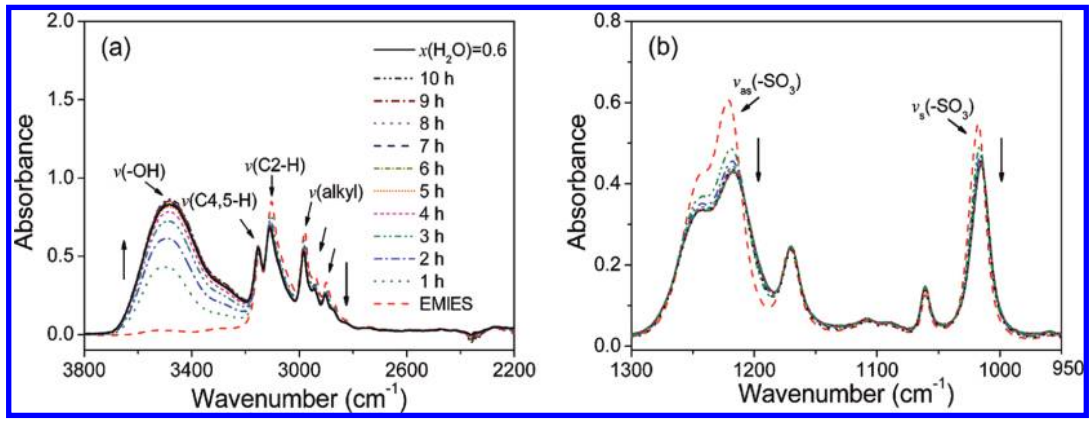

Figure 3. ATR-IR spectra as functions of time (hours), showing changes of various absorbance bands of EMIES as labeled in the figure upon water uptake from air. ZnSe (a) and Ge (b) ATR crystals were used. The solid lines are the spectra of aqueous EMIES at $x(H_2O) = 0.6$ (10.25 wt %).

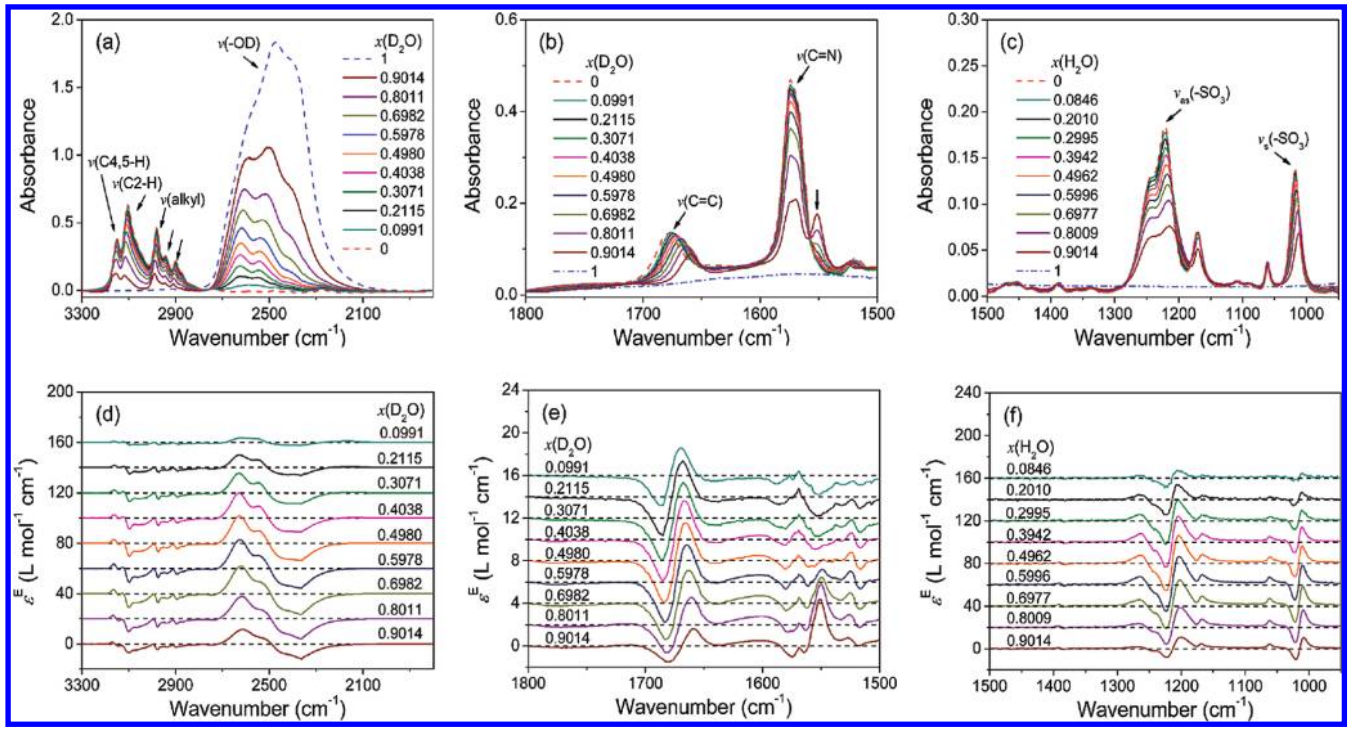

Figure 4. Infrared (upper) and excess infrared (lower) spectra of the EMIES−D_2O system in the range of the alkyl and −OD stretching vibration (a and d), the C═C and C═N stretching vibration (b and e), and the $-SO_3$ stretching vibration (c and f).

process, in agreement with the general understanding that S═O is a very good proton acceptor in forming H-bonds with water molecules.

The excess molar absorbances of C4,5−H, C2−H, and $-SO_3$ stretching vibration at different water concentrations are displayed in Figure 5b. $\nu_s(-SO_3)$ and $\nu_{as}(-SO_3)$ have positive

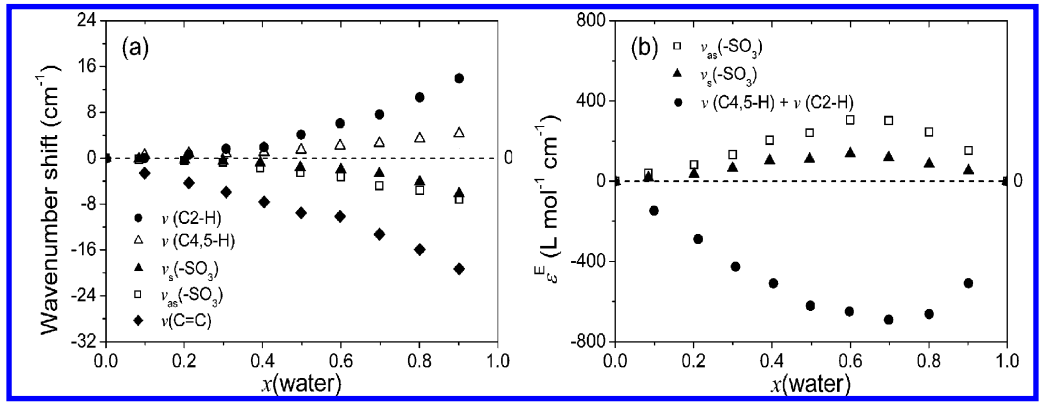

Figure 5. Wavenumber shift of C4,5−H, C2−H, $-SO_3$, and C═C stretching vibrations (a) and excess molar absorbance of (C4,5−H + C2−H) and $-SO_3$ stretching vibrations (b) at different concentrations of water. D_2O was used to examine almost all of the IR bands except the bands of $-SO_3$ where H_2O was the solvent.

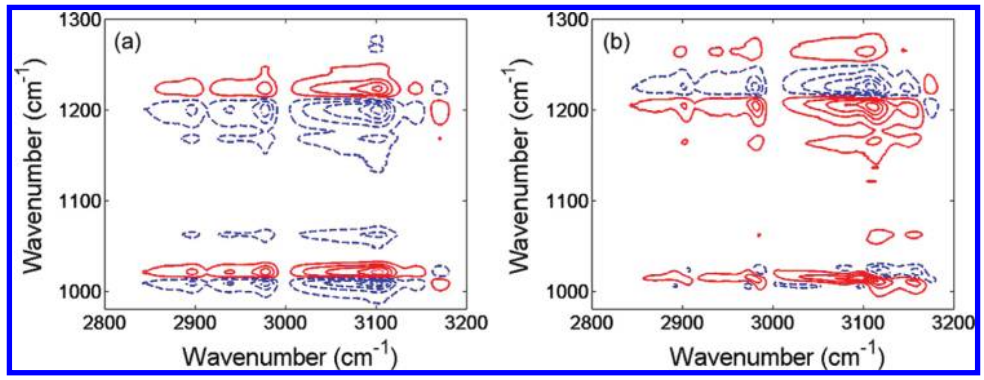

Figure 6. Synchronous (a) and asynchronous (b) 2D correlation contour maps of C−H and $-SO_3$ stretching vibrations in the dilution process by water.

excess molar absorbance, while ν(C2−H) and ν(C4,5−H) have negative excess molar absorbance. As judged by the general understanding of the common red-shifted H-bonds,[60] the increase or decrease in infrared absorbance is explained as a result of the strengthening or weakening of hydrogen bonds. The excess molar absorbance reported here further supports our conclusions on the H-bond interactions in the dilution process as discussed above. Namely, the hydrogen bond involving $-SO_3$ is enhanced (positive excess molar absorbance) and that involving the C−H in the imidazolium ring is weakened upon dilution (negative excess molar absorbance). The different changing patterns in hydrogen bond strength as discussed above suggest the possible existence of selective interactions among water, anion, and acidic protons on the imidazolium ring.

3.2. Two-Dimensional Correlation Analysis. In order to probe the sequential order of interactions in the dilution process of EMIES by water, 2D correlation analysis is performed with focus on ν(alkyls) and $\nu(-SO_3)$ in EMIES with increasing water concentration. Since the bands of ν(alkyls) are overlapped by the stretching vibration of H_2O and the bands of $\nu(-SO_3)$ are overlapped by the bending vibration of D_2O, the ν(alkyls) in the EMIES−D_2O system and $\nu(-SO_3)$ in the EMIES−H_2O system are used to do the 2D correlation analysis. These selected bands were normalized with the modified component-normalization method;[39] i.e., the absorption bands of ν(alkyls) and $\nu(-SO_3)$ in excess infrared spectra were divided by the corresponding mole fraction of EMIES. The synchronous and asynchronous 2D correlation contour maps of ν(alkyl) and $\nu(-SO_3)$ in the EMIES−water system are given in Figure 6. Take the cross peaks of ν(C2−H) located at 3104 cm^{-1} and $\nu_s(-SO_3)$ located at 1018 cm^{-1} as an example. There are two cross peaks at (3106 cm^{-1}, 1007 cm^{-1}) and (3103 cm^{-1}, 1021 cm^{-1}) in the synchronous 2D correlation map and also two cross peaks at (3116 cm^{-1}, 1010 cm^{-1}) and (3116 cm^{-1}, 1023 cm^{-1}) in the asynchronous 2D correlation map. In the synchronous 2D correlation map, the cross peak at (3106 cm^{-1}, 1007 cm^{-1}) is negative and that at (3103 cm^{-1}, 1021 cm^{-1}) is positive. The negative or positive peaks are due to the different or same changing directions of the absorption coefficient of ν(C2−H) and $\nu_s(-SO_3)$. The changing direction of the absorption coefficient can be indicated by the excess infrared spectra (Figure 4d,f): the excess mole absorbance of ν(C2−H) is negative, while the excess mole absorbance of $\nu_s(-SO_3)$ is negative at higher wavenumber and positive at lower wavenumber. In the asynchronous 2D correlation map, the cross peak at (3116 cm^{-1}, 1010 cm^{-1}) is positive and that at (3116 cm^{-1}, 1023 cm^{-1}) is negative. Thus, the signs of synchronous and asynchronous cross peaks of [ν(C2−H), $\nu_s(-SO_3)$] are different. According to Noda's rule,[45,46] the absorption coefficient of $\nu_s(-SO_3)$ varies prior to that of ν(C2−H) with increasing concentration of water. The signs of synchronous and asynchronous cross peaks of [ν(C2−H), $\nu_{as}(-SO_3)$], [ν(C4,5−H), $\nu_s(-SO_3)$], and [ν(C4,5−H), $\nu_{as}(-SO_3)$] are also different, indicating the absorption coefficient of $-SO_3$ stretching vibration varies prior to that of C2−H and C4,5−H stretching vibration with increasing water concentration. Namely, the water molecule interacts preferentially with the $-SO_3$ group of EMIES.

Furthermore, the selective interaction of H_2O with the $-SO_3$ group may be responsible for the previous deduction that the imidazolium ring may undergo a different interaction when $x(H_2O) \geq 0.6$ with the increase of water content. The dynamic process is proposed as follows: water molecules interact first with the $-SO_3$ group, leading to the weakening of the hydrogen bond between 1-ethyl-3-methylimidazolium cation and ethyl sulfate anion; then, water molecules interact with the C−H groups in the imidazolium ring directly when $x(H_2O) \geq 0.6$, leading to an evident change of the C=N stretching vibration.

Considering the shape change and peak shift may influence proper 2D correlation analysis, we have used a parameter, relative extent of absorbance variation η, to evaluate the selective interactions separately. The parameter η and the deviation of absorption coefficient ε_d have been described elsewhere.[39,41] Their expressions are as follows.

$$\varepsilon_d = \frac{\varepsilon^E}{x_1} \tag{2}$$

$$\eta = \frac{\varepsilon_d}{\varepsilon_{d,ref}} \tag{3}$$

where $\varepsilon_{d,ref}$ is a selected reference value of ε_d at a high enough water concentration. The integral values of ε_d for ν(C4,5−H) + ν(C2−H) and $\nu_{as}(-SO_3)$ and $\nu_s(-SO_3)$ are shown in Figure 7a. The ε_d value of ν(C4,5−H) + ν(C2−H) is negative, and those of $\nu_{as}(-SO_3)$ and $\nu_s(-SO_3)$ are all positive and change monotonously with increasing water concentration.

By taking x(water) = 0.9 as the reference point, the relative extents of absorbance variation of ν(C4,5−H) + ν(C2−H), $\nu_s(-SO_3)$, and $\nu_{as}(-SO_3)$ are calculated. The results are shown in Figure 7b. Both of the curves for $\nu_s(-SO_3)$ and $\nu_{as}(-SO_3)$ have a shorter half-time and a greater half-intensity than that of ν(C4,5−H) + ν(C2−H) in EMIES with increasing D_2O or H_2O concentration. This means that the $-SO_3$ group in EMIES changes in precedence to the C−H group in EMIES with increasing water concentration.[48] The results demonstrate that the interaction of H_2O with $-SO_3$ in the anion of EMIES is

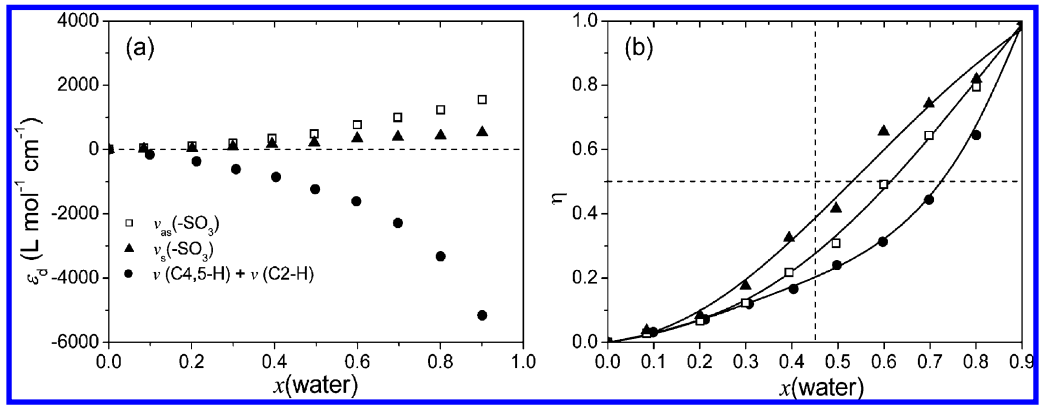

Figure 7. Absorbance deviation (a) and a parameter express the relative extent of absorbance variation (b) of C4,5−H, C2−H, and −SO_3 stretching vibrations at different concentrations of D_2O or H_2O.

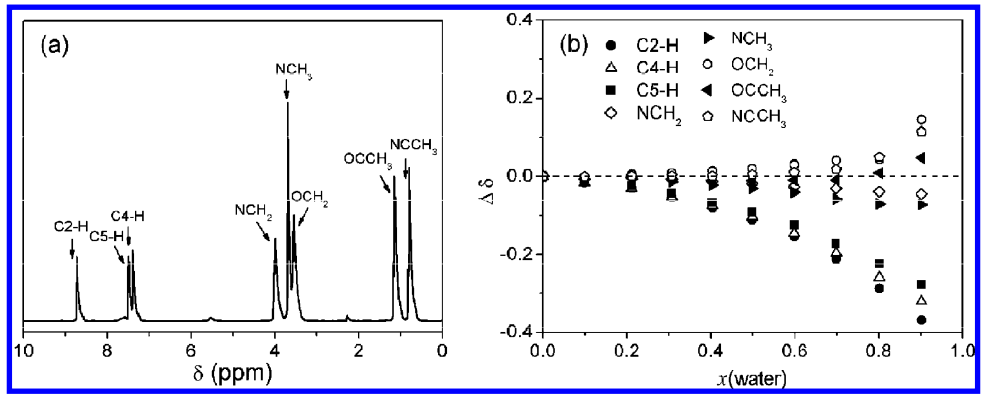

Figure 8. ^{1}H NMR (a) of pure EMIES and chemical shift difference (b) of hydrogen atoms in EMIES in the dilution process by D_2O.

stronger than that with the C−H groups of the imidazolium cation, resulting in a preferential change in the absorption coefficient of $\nu_s(-SO_3)$ and $\nu_{as}(-SO_3)$. These results are in agreement with the conclusions drawn from 2D correlation analysis.

3.3. ^{1}H NMR Chemical Shift Analysis. ^{1}H NMR measurements of pure EMIES and EMIES−D_2O mixtures were carried out at 298 K, and the chemical shift changes of individual hydrogen atoms during the dilution process were evaluated. The ^{1}H NMR chemical shift data are listed in Table SI1 in the Supporting Information. The chemical shift changes of individual hydrogen atoms are displayed in Figure 8. The results show that the chemical shifts of C2−H, C4−H, and C5−H have the most significant changes and they move to a high field position upon dilution. This indicates an increased electron density of these three hydrogen atoms, a result of the weakening of the hydrogen bonding interactions. The chemical shifts of hydrogen atoms in NCH_2 and NCH_3 show a slight upfield chemical shift, and those of OCH_2, OCH_2CH_3 (or simplified as $OCCH_3$), and NCH_2CH_3 (or $NCCH_3$) are shifted downfield, resulting probably from the influence of hydrogen bonding cooperativity. The chemical shift information confirms the conclusions drawn from IR studies, showing that the hydrogen bonding involving C−H groups in the dialkyl-imidazolium ring becomes weaker with increasing water concentration.

3.4. Quantum Chemical Calculations. The optimized geometries of EMIES, 1-ethyl-3-methylimidazolium cation (EMI)−H_2O, and ethyl sulfate anion (ES)−H_2O were studied. The results are shown in Figure 9a−c. The sum of van der Waals atomic radii of hydrogen and oxygen (2.5 Å) is used as a critical value for judging if a hydrogen bond is present between hydrogen and oxygen atoms.[61] Hydrogen bonds are denoted by dashed lines, and the corresponding H···O distances are labeled

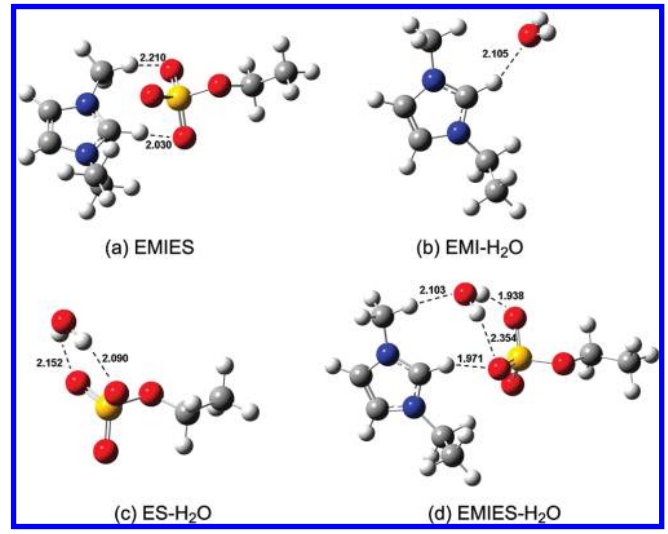

Figure 9. Optimized geometries of EMIES and possible positions for water molecules interacting with EMIES: (a) EMIES; (b) EMI cation and H_2O; (c) ES anion and H_2O; (d) EMIES and H_2O. Hydrogen bonds are denoted by dashed lines, and the corresponding H···O distances are labeled.

in Figure 9. It is found that hydrogen bonds can exist between C2−H or alkyl C−H and O═S in EMIES, between C2−H and O in EMI−H_2O, and between O−H and O═S in ES−H_2O. It is noteworthy that both the anion ES (Figure 9a) and water molecule (Figure 9b) prefer to interact with C2−H, rather than with C4,5−H. Comparison of the interaction pairs in Figure 9a and b tells us that, though the bigger size donor ES can form a H-bond with C2−H and CH_3, the smaller size donor H_2O can only form a H-bond with C2−H. These results suggest that C2−H is the most active hydrogen atom in the cation, consistent

TABLE 2: Interaction Energies (ΔE, kJ/mol), Stretch Frequencies (ν, cm^{-1}), and Intensities (I, km/mol) of the C−H Groups in the Dialkyl-Imidazolium Ring and $-SO_3$ in the Ethyl Sulfate Anion in the Complexes of EMIES, EMI−H_2O, and ES−H_2O

	EMIES	EMI−H_2O	ES−H_2O
ΔE	−362.03	−48.36	−59.67
ν_s(C4,5−H) (I)	3165 (2)	3162 (10)	
ν_{as}(C4,5−H) (I)	3148 (6)	3146 (14)	
ν(C2−H) (I)	3043 (313)	3080 (208)	
$\nu_{as}(-SO_3)$ (I)	1161 (284)		1124 (312)
$\nu_s(-SO_3)$ (I)	940 (269)		937 (200)

with the facts that the carbon C2 is positively charged owing to the electron deficit in the imidazolium ring, making C2−H the most acidic hydrogen atom on the imidazolium ring.[5,34]

The interaction energies of EMIES, EMI−H_2O, and ES−H_2O and the stretching frequencies and vibration intensities of the respective functional groups are summarized in Table 2. It can be seen that the interaction energy of EMIES (−362.03 kJ/mol) is much larger in absolute value than that of EMI−H_2O (−48.36 kJ/mol) and ES−H_2O (−59.67 kJ/mol), respectively. The large interaction energy of EMIES is due to the electrostatic interaction of the cation and the anion. The interaction energy of ES−H_2O is greater than that of EMI−H_2O, indicating that the interaction between H_2O and the ethyl sulfate anion is stronger than that between H_2O and the 1-ethyl-3-methylimidazolium cation. This is in agreement with the FTIR results, where ν(C2−H) shows a blue shift and decreased intensity, while $\nu_{as}(-SO_3)$ and $\nu_s(-SO_3)$ are red-shifted and increased in intensity in the presence of water. Due to the larger interaction energy, water molecules may selectively interact with the ethyl sulfate anion under low hydration conditions. Furthermore, the interaction energy of EMIES−H_2O (−413.56 kJ/mol) is larger in absolute value than that of EMIES (−362.03 kJ/mol). This explains the ready solubility of EMIES in water and the hygroscopic property of this ionic liquid.

Neither cation EMI nor anion ES can exist alone in a system. However, the interaction models depicted in Figure 9b and c are provided for the understanding of the selective interaction between water and the cation/anion of EMIES. The shorter hydrogen bond length between SO and H_2O than that between C2−H and OH_2 supports our conclusion that the main interaction site of the water molecule in the EMIES−H_2O system is the ethyl sulfate anion at low water concentration.

The optimized geometry of an EMIES−H_2O complex has also been evaluated, and the result is shown in Figure 9d. This gives the anion−water interaction mode in the presence of cation. It is found that hydrogen bonding interactions are present between H_2O and two oxygen atoms of the $-SO_3$ group in the ethyl sulfate anion with the O···H distances of 1.938 and 2.354 Å, respectively. A H-bond is also present between the $-SO_3$ group and the C2−H on the imidazolium ring with an O···H distance of 1.971 Å. The O···H distance between H_2O and C2−H on the imidazolium ring is 2.777 Å, longer than the sum of van der Waals radii of H and O elements, demonstrating that no hydrogen bonding interaction is present between H_2O and the C2−H group on the imidazolium ring at this water−IL composition. We note that the O···H distance between the oxygen atom of H_2O and one hydrogen of the $-CH_3$ group on the side chain of the cation is very short (2.103 Å), indicating the possible existence of a H-bond between H_2O and the alkyl chain of 1-ethyl-3-methylimidazolium cation, which is usually weaker than that between H_2O and the aromatic C−H.[34,58] The reason that water forms H-bonds with the methyl C−H, rather than aromatic C2−H, is explained as the presence of strong cation−anion interaction.

Finally, it is noteworthy that Figure 9 gives only some probable geometries of interaction complexes in the mixture of EMIES and water. Those cannot represent all of the possible interaction modes over the wide water concentration range. Taking low water content as an example, Köddermann et al.[4] reported that a water molecule forms two H-bonds to two anions in the EMIES−water binary system, while it forms two H-bonds with one anion when the ethyl sulfate anion is replaced with bis(trifluoromethylsulfonyl)imide (NTf_2). Using the molecular dynamics method, Porter et al.[37] demonstrated that the interaction mode in the latter case is also anion−water−anion, which is in agreement with an earlier experimental work of Cammarata et al.[36] At high water content, we believe self-associated water molecules, ion−water interaction complexes with ratios different from 1/1, and the cooperative H-bonding networks such as the ES−water−water complex also exist in the studied system. Even some thermodynamically unstable interaction modes can be present in the system kinetically. All of these forms of interactions jointly give the broad feature of OH (OD) stretching vibration as observed in IR spectra.

Conclusions

ATR-IR spectra of the EMIES−water binary system with different mole fractions of water show the influence of water content on the mode and intensity of hydrogen bonding interactions between water molecules and the cation/anion of EMIES. The C−H groups in the dialkyl-imidazolium ring and $-SO_3$ in the ethyl sulfate anion are characteristic groups interacting with water molecules. Using excess infrared spectroscopy, it was found that the $-SO_3$ group in the ethyl sulfate anion undergoes enhanced hydrogen bonding interaction and the C−H groups in the 1-ethyl-3-methylimidazolium cation undergo weakened hydrogen bonding interaction with the increasing concentration of water. The analysis of theoretical calculations and chemical shift difference in ^{1}H NMR also supports these results. Two-dimensional correlation analysis demonstrates that the hydrogen bonding interaction between H_2O and $-SO_3$ is prior to the interaction between H_2O and the C−H group on the imidazolium ring during the hydration process. Water, at limiting concentrations, interacts preferentially with the ethyl sulfate anion. At high concentrations, namely, when the mole fraction is $x \geq 0.6$ as evidenced from the infrared and excess spectra, water can also interact with the hydrogen atoms on the imidazolium ring, forming a stable new complex. Through comparison of the mutual interactions among the species EMI, ES, and water, the following sequential order of interaction strength is obtained: EMI−water−ES > EMI−ES > ES−water > EMI−water. These studies on hydrogen bonding interactions between EMIES and water provide important information for a deeper understanding of the physical properties of the sulfate-containing ILs and may shed light on the application of this family of ionic liquids.

Acknowledgment. This work was supported by the Natural Science Foundation of China (Project Nos. 20633080 and 20973100) and a "973" National Key Basic Research Program of China (Grant No. 2006CB806203).

Supporting Information Available: Table showing the H-NMR chemical shifts of EMIES at different water concentrations. This material is available free of charge via the Internet at http://pubs.acs.org.

References and Notes

(1) Rogers, R. D., Seddon, K. R., Eds. *Ionic Liquids Industrial Applications for Green Chemistry*; ACS Symposium Series 818; American Chemical Society: Washington, DC, 2002.

(2) Rogers, R. D., Seddon, K. R., Eds. *Ionic Liquids as Green Solvent*; ACS Symposium Series 856; American Chemical Society: Washington, DC, 2003; Chapter 12.

(3) Rogers, R. D., Seddon, K. R., Eds. *Ionic Liquids IIIA: Fundamentals, Progress, Challenges, and Opportunities: Properties and Structure*; American Chemical Society: Washington, DC, 2005; Vol. 901.

(4) Köddermann, T.; Wertz, C.; Heintz, A.; Ludwig, R. *Angew. Chem., Int. Ed.* **2006**, *45*, 3697–3702.

(5) Fumino, K.; Wulf, A.; Ludwig, R. *Angew. Chem., Int. Ed.* **2008**, *47*, 8731–8734.

(6) Dupont, J.; de Souza, R. F.; Suarez, P. A. Z. *Chem. Rev.* **2002**, *102*, 3667–3692.

(7) Macfarlane, D. R.; Seddon, K. R. *Aust. J. Chem.* **2007**, *60*, 3–5.

(8) Zhao, H.; Xia, S.; Ma, P. *J. Chem. Technol. Biotechnol.* **2005**, *80*, 1089–1096.

(9) Earle, M.; Forestier, A.; Olivier-Bourbigou, H.; Wasserscheid, P. In *Ionic Liquids in Synthesis*; Wasserscheid, P., Welton, T., Eds.; Wiley-VCH Verlag: Weinheim, Germany, 2003.

(10) Jain, N.; Kumar, A.; Chauhan, S.; Chauhan, S. M. S. *Tetrahedron* **2005**, *61*, 1015–1060.

(11) Krossing, I.; Slattery, J. M. *Z. Phys. Chem.* **2006**, *220*, 1343–1359.

(12) Holbrey, J. D.; Reichert, W. M.; Swatloski, R. P.; Seddon, K. R.; Rogers, R. D. *Green Chem.* **2002**, *4*, 407–413.

(13) Borra, E. F.; Seddiki, O.; Angel, R.; Eisenstein, D.; Hickson, P.; Seddon, K. R.; Worden, S. P. *Nature* **2007**, *447*, 979–981.

(14) Torrecilla, J. S.; Rojo, E.; García, J.; Rodríguez, F. *Ind. Eng. Chem. Res.* **2008**, *47*, 4025–4028.

(15) Ficke, L. E.; Rodríguez, H.; Brennecke, J. F. *J. Chem. Eng. Data* **2008**, *53*, 2112–2119.

(16) González, E. J.; González, B.; Calvar, N.; Domínguez, A. *J. Chem. Eng. Data* **2007**, *52*, 1641–1648.

(17) Torrecilla, J. S.; Rafione, T.; García, J.; Rodríguez, F. *J. Chem. Eng. Data* **2008**, *53*, 923–928.

(18) Rodríguez, H.; Brennecke, J. F. *J. Chem. Eng. Data* **2006**, *51*, 2145–2155.

(19) Fröba, A. P.; Wasserscheid, P.; Gerhard, D.; Kremer, H.; Leipertz, A. *J. Phys. Chem. B* **2007**, *111*, 12817–12822.

(20) Heintz, A. *J. Chem. Thermodyn.* **2005**, *37*, 525–535.

(21) Kelkar, M. S.; Shi, W.; Maginn, E. J. *Ind. Eng. Chem. Res.* **2008**, *47*, 9115–9126.

(22) Tong, J.; Liu, Q. S.; Xu, W. G.; Fang, D. W.; Yang, J. Z. *J. Phys. Chem. B* **2008**, *112*, 4381–4386.

(23) Wang, J. F.; Li, C. X.; Wang, Z. H. *J. Chem. Eng. Data* **2007**, *52*, 1307–1312.

(24) Widegren, J. A.; Saurer, E. M.; Marsh, K. N.; Magee, J. W. *J. Chem. Thermodyn.* **2005**, *37*, 569–575.

(25) Widegren, J. A.; Laesecke, A.; Magee, J. W. *Chem. Commun.* **2005**, *12*, 1610–1612.

(26) Heintz, A.; Lehmann, J. K.; Wertz, C.; Jacquemin, J. *J. Chem. Eng. Data* **2005**, *50*, 956–960.

(27) Najdanovic-Visak, V.; Rebelo, L. P. N.; da Ponte, M. N. *Green Chem.* **2005**, *7*, 443–450.

(28) Elaiwi, A.; Hitchcock, P. B.; Sedden, K. R.; Srinivasan, N.; Tan, Y. M.; Welton, T.; Zora, J. A. *J. Chem. Soc., Dalton Trans.* **1995**, *21*, 3467–3472.

(29) Jiang, W.; Wang, Y.; Voth, G. A. *J. Phys. Chem. B* **2007**, *111*, 4812–4818.

(30) Takamuku, T.; Kyoshoin, Y.; Shimomura, T.; Kittaka, S.; Yamaguchi, T. *J. Phys. Chem. B* **2009**, *113*, 10817–10824.

(31) Fumino, K.; Wulf, A.; Ludwig, R. *Angew. Chem., Int. Ed.* **2009**, *48*, 3184–3186.

(32) Köddermann, T.; Paschek, D.; Ludwig, R. *ChemPhysChem* **2008**, *9*, 549–555.

(33) Köeddermann, T.; Wertz, C.; Heintz, A.; Ludwig, R. *ChemPhysChem* **2006**, *7*, 1944–1949.

(34) Zhang, L. Q.; Wang, Y.; Xu, Z.; Li, H. R. *J. Phys. Chem. B* **2009**, *113*, 5978–5984.

(35) Chang, H. C.; Jiang, J. C.; Tsai, W. C.; Chen, G. C.; Lin, S. H. *J. Phys. Chem. B* **2006**, *110*, 3302–3307.

(36) Cammarata, L.; Kazarian, S. G.; Salterb, P. A.; Welton, T. *Phys. Chem. Chem. Phys.* **2001**, *3*, 5192–5200.

(37) Porter, A. R.; Liem, S. Y.; Popelier, P. L. A. *Phys. Chem. Chem. Phys.* **2008**, *10*, 4240–4248.

(38) Lasségues, J. C.; Grondin, J.; Cavagnat, D.; Johansson, P. *J. Phys. Chem. A* **2009**, *113*, 6419–6421.

(39) Wang, N. N.; Jia, Q.; Li, Q. Z.; Yu, Z. W. *J. Mol. Struct.* **2008**, *883−884*, 55–60.

(40) Wang, N. N.; Li, Q. Z.; Yu, Z. W. *Appl. Spectrosc.* **2009**, *63*, 1356–1362.

(41) Li, Q. Z.; Wang, N. N.; Zhou, Q.; Sun, S. Q.; Yu, Z. W. *Appl. Spectrosc.* **2008**, *62*, 166–170.

(42) Li, Q. Z.; Wu, G. S.; Yu, Z. W. *J. Am. Chem. Soc.* **2006**, *128*, 1438–1439.

(43) Koga, Y.; Sebe, F.; Minami, T.; Otake, K.; Saitow, K.; Nishikawa, K. *J. Phys. Chem. B* **2009**, *113*, 11928–11935.

(44) Zhang, L. Q.; Xu, Z.; Wang, Y.; Li, H. R. *J. Phys. Chem. B* **2008**, *112*, 6411–6419.

(45) Noda, I. *Appl. Spectrosc.* **1993**, *47*, 1329–1336.

(46) Noda, I.; Ozaki, Y. *Two-Dimensional Correlation Spectroscopy: Applications in Vibrational and Optical Spectroscopy*; Wiley: Chichester, U.K., 2004; pp 22−23.

(47) Czarnik-Matusewicz, B.; Bin Kim, S.; Jung, Y. M. *J. Phys. Chem. B* **2009**, *113*, 559–566.

(48) Jia, Q.; Wang, N. N.; Yu, Z. W. *Appl. Spectrosc.* **2009**, *63*, 344–353.

(49) Noda, I.; Dowrey, A. E.; Marcott, C.; Story, G. M.; Ozaki, Y. *Appl. Spectrosc.* **2000**, *54*, 236A–248A.

(50) Noda, I.; Liu, Y.; Ozaki, Y. *J. Phys. Chem.* **1996**, *100*, 8674–8680.

(51) Yang, J. Z.; Wang, B.; Zhang, Q. G.; Tong, J. *Fluid Phase Equilib.* **2007**, *251*, 68–70.

(52) Hansen, W. N. *Spectrochim. Acta* **1965**, *21*, 815–833.

(53) Frisch, M. J.; Trucks, G. W.; Schlegel, H. B.; Scuseria, G. E.; Robb, M. A.; Cheesman, J. R.; Zakrzewski, V. G.; Montgomery, J. A., Jr.; Stratmann, R. E.; Burant, J. C.; Dapprich, S.; Millam, J. M.; Daniels, A. D.; Kudin, K. N.; Strain, M. C.; Farkas, O.; Tomasi, J.; Barone, V.; Cossi, M.; Cammi, R.; Mennucci, B.; Pomelli, C.; Adamo, C.; Clifford, S.; Ochterski, J.; Petersson, G. A.; Ayala, P. Y.; Cui, Q.; Morokuma, K.; Malick, D. K.; Rabuck, A. D.; Raghavachari, K.; Foresman, J. B.; Cioslowski, J.; Ortiz, J. V.; Baboul, A. G.; Stefanov, B. B.; Liu, G.; Liashenko, A.; Piskorz, P.; Komaromi, I.; Gomperts, R.; Martin, R. L.; Fox, D. J.; Keith, T.; Al-Laham, M. A.; Peng, C. Y.; Nanayakkara, A.; Gonzalez, C.; Challacombe, M.; Gill, P. M. W.; Johnson, B.; Chen, W.; Wong, M. W.; Andres, J. L.; Gonzalez, C.; Head-Gordon, M.; Replogle, E. S.; Pople, J. A. *Gaussian 03*, revision B.03; Gaussian, Inc.: Pittsburgh, PA, 2003.

(54) Dhumal, N. R.; Kim, H. J.; Kiefer, J. *J. Phys. Chem. A* **2009**, *113*, 10397–10404.

(55) Talaty, E. R.; Raja, S.; Storhaug, V. J.; Dolle, A.; Carper, W. R. *J. Phys. Chem. B* **2004**, *108*, 13177–13184.

(56) Izgorodina, E. I.; Bernard, U. L.; MacFarlane, D. R. *J. Phys. Chem. A* **2009**, *113*, 7064–7072.

(57) Kiefer, J.; Fries, J.; Leipertz, A. *Appl. Spectrosc.* **2007**, *61*, 1306–1311.

(58) Joseph, J.; Jemmis, E. D. *J. Am. Chem. Soc.* **2007**, *129*, 4620–4632.

(59) Fawcett, W. R.; Kloss, A. A. *J. Phys. Chem. B* **1996**, *100*, 2019–2024.

(60) Iogansen, A. V. *Spectrochim. Acta, Part A* **1999**, *55*, 1585–1612.

(61) Pauling, L. *The Nature of the Chemical Bond*, 3rd ed.; Cornell University Press: New York, 1960.

JP1009498